1 THE HYDRODYNAMIC MODEL

The hydrodynamical model used in this paper is a three-dimensional time-dependent numerical simulation of an HMXB first presented by Owen & Blondin (1997). The parameters of this model were chosen in accordance with the observed parameters of LMC X-4 (see Table 1). The high X-ray luminosity of LMC X-4 is difficult to reconcile with wind accretion alone, and the presence of a 30 day period in the X-ray light curve (Lang et al. 1981) and in the optical light curve (Heemskerk & van Paradijs 1989) suggests a precessing accretion disk fed by Roche lobe overflow.

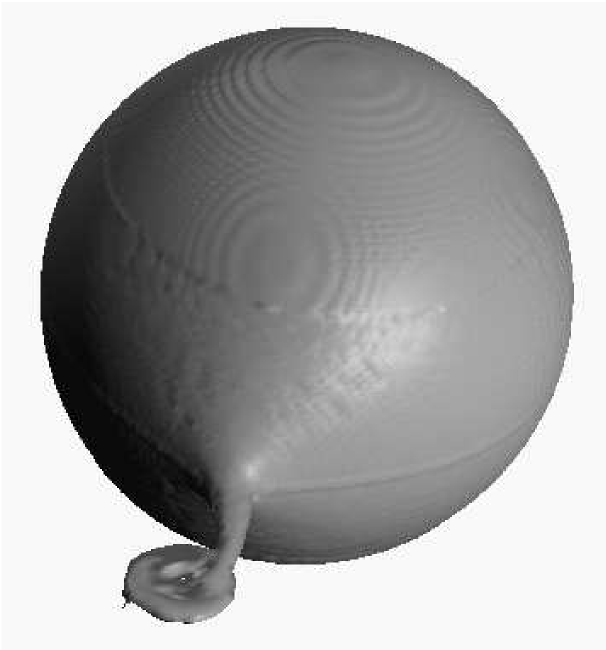

Figure 1: An isodensity surface of the hydrodynamic model at the end of the numerical simulation, illustrating the relative scales of the accretion disk, tidal stream and primary star.

1.1 Numerical Method

Our numerical model is an extension of previous models (Blondin et al.1990, Blondin et al.1991, Blondin 1994, Blondin & Woo 1995) used to study the dynamics of the circumstellar gas in HMXBs, and in particular the disruption of the normal OB stellar wind by the compact X-ray source. These models are based on the time-dependent hydrodynamics code VH-1, and include (1) a radiatively driven stellar wind incorporated via the Sobolev approximation, (2) the X-ray photoionization of the wind as approximated by a cutoff of the radiative driving force, and (3) the X-ray heating and radiative cooling of the circumstellar gas.

The principle modification to this current model over that used in Blondin & Woo (1995) is the inclusion of the gravity of the compact X-ray source. This adds several features to the model, including tidal distortion of the primary, Roche lobe overflow leading to the formation of a tidal stream, the presence of an accretion disk, and a realistic mass accretion rate. In order to accurately model these features the spherical numerical grid (188 by 63 by 201 zones in r, θ, and ϕ) was structured to provide the highest spatial resolution near the surface of the distorted primary and near the accreting compact object.

The model is evolved only in one hemisphere, assuming reflection symmetry about the equatorial plane. In addition, a cone about the polar axis is removed from the simulation to reduce the number of time steps needed in the simulation. The use of an explicit hydrodynamics code restricts the time step to the smallest value of $\Delta x/v$ on the grid, where Δx is the width of a numerical zone, and v is a characteristic velocity (either the gas velocity or the sound speed). On a spherical grid Δx in the ϕ direction is given by $r \sin\theta\, \Delta\phi$. Therefore, as $\theta \to 0$, the zone width $\Delta x \to 0$ and $\Delta t \to 0$. Thus, to keep a reasonable value of Δt, we limited the simulation domain to $\theta > 0.3\pi$.

The numerical simulation was initialized with the surface of the primary star just inside the critical potential surface, such that the effective potential at the stellar surface was greater than the critical potential by one part in 10^5. The boundary conditions on this surface correspond to an isothermal atmosphere in hydrostatic equilibrium. At the stellar surface temperature of 4×10^4 K, the scale height in this atmosphere is $\sim 10^9$ cm. From numerical experiments we found that VH-1 could simulate a stable atmosphere with zone spacing as large as twice the scale height; this is the value used in the present model. The density at this boundary is set at 5×10^{-9} g cm^{-3}, a value determined emperically to produce a stable stellar wind with the given parameters. The parameters describing the radiative driving force ($\alpha = 0.53$, $k = 0.12$; see e.g., Castor, Abbott & Klein 1975) were chosen based on the spectral type of the primary star. In the absence of a companion, this model would drive a spherical stellar wind with a mass loss rate of $\dot{M}_w \approx 2 \times 10^{-7}\,\mathrm{M_\odot\,yr^{-1}}$ and a terminal wind velocity of $v_\infty \approx 2000$ km s^{-1}.

The accretion-driven X-ray flux photo-ionizes, heats, and imparts momentum to the circumstellar gas. The X-ray luminosity was computed self-consistently as a function of the mass accretion rate onto the compact companion: $L_x = 0.1\dot{M}c^2$. This mass accretion rate, $\dot{M}$, was computed by removing mass and energy from a block of 3^3 zones at the location of the companion (the zone size at this location is $\Delta x = 2.5 \times 10^9$ cm). However, the dense gas of the tidal stream and accretion disk are expected to be highly optically thick, and will shadow other regions of the binary system from this intense X-ray flux. To account for this shadowing in the simplest fashion, we computed the optical depth from the compact X-ray source to each numerical zone, and reduced the X-ray flux by $e^{-\tau}$. The reduced flux was used to calculate the local photoionization parameter, X-ray heating, and X-ray radiation pressure.

1.2 Simulation Results

The simulation was evolved for approximately one binary orbital period. This was sufficient time for the accretion disk to circularize and for the circumstellar gas to reach a state of quasi-equilibrium. By the end of the simulation there were five key features of the circumstellar gas: a radiatively driven wind from the shadowed surface of the primary star, a wind-compressed disk created by the rapid rotation of the primary star, a tidal stream emanating from the inner Lagrange point (L1), a Keplerian accretion disk around the compact object, and an X-ray irradiation driven wind emanating from the inner regions of the accretion disk.

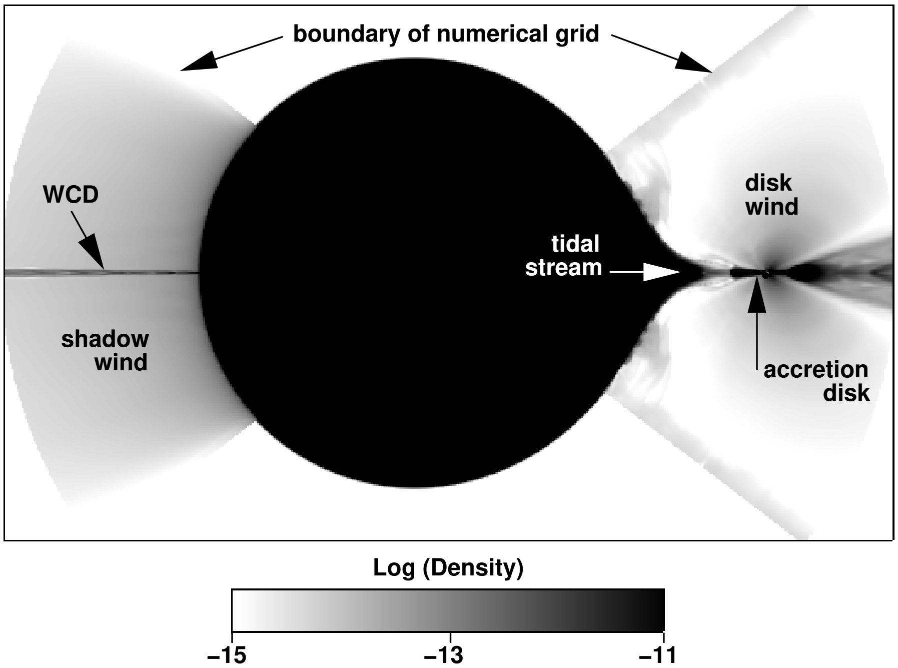

Figure 2: A two-dimensional slice along the line of centers of the binary system illustrating the five key components of the circumstellar gas.

The radiatively driven O-star wind fills a large fraction of the binary system due to the strong shadowing effects of the accretion disk. This normal stellar wind is marked by the presence of a wind-compressed disk (Bjorkman & Cassinelli 1993). The density of the wind in the equatorial plane is a factor of ~ 20 higher than at other latitudes. This effect is a direct result of assuming co-rotation between the primary star and the binary system; A slower stellar rotation would diminish or remove the wind-compressed disk.

The tidal stream is described remarkably well by the analysis of Lubow & Shu (1975). The tidal stream leaves the L1 point with an angle of $\sim 25^{\circ}$, in good agreement with the analytic prediction. The stream becomes supersonic only 10^{10} cm downstream, with the centroid of the stream following a ballistic trajectory until the stream impacts the disk. The gas in the stream continues to accelerate, reaching a Mach number at impact of ~ 16.

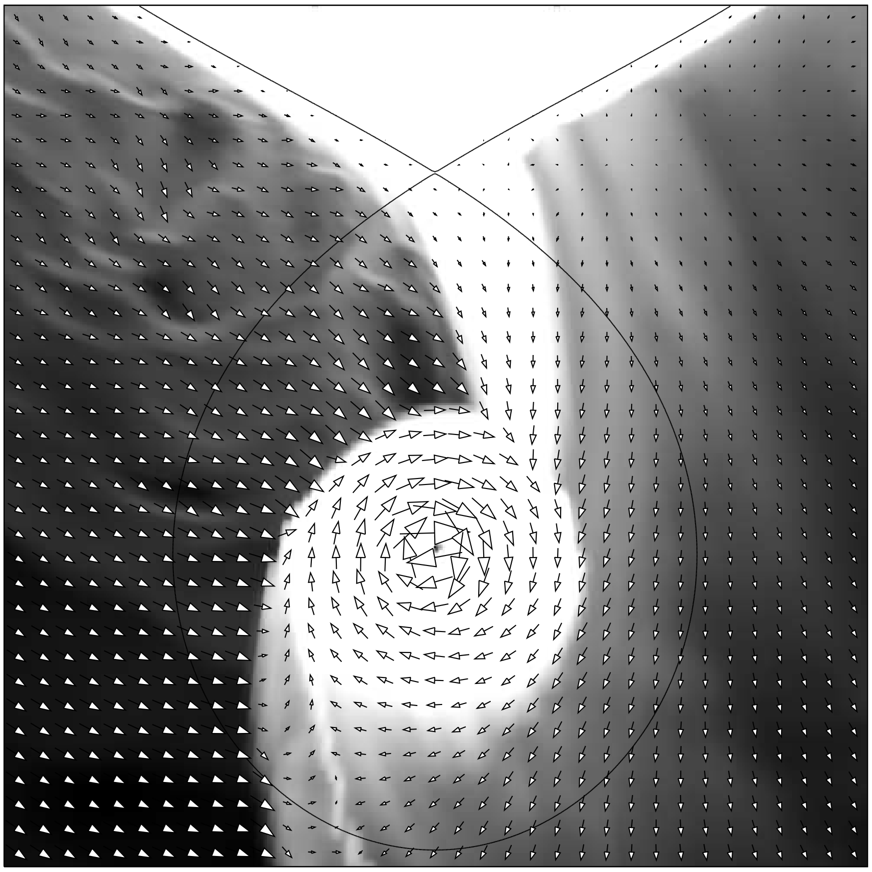

Figure 3: The velocity field of the circumstellar gas in the equatorial plane of the binary system. Here black represents the relatively low density of the equatorial wind, while white represents the high density of the primary star, tidal stream, and accretion disk. The solid line marks the critical potential surface.

The width of the tidal stream ($\sim 7 \times 10^{10}$ cm) is in good agreement with Lubow & Shu (1975); 70 % of the stream mass flux is within their quoted width. The stream cross section is consitently oblate, with the stream width being about 4/3 of the stream height. As shown by Lubow & Shu (1976), the vertical structure of the stream is determined entirely by the foot points of the streamlines in the tidal stream, and hence the stream has a scale height much larger than that expected for hydrostatic equilibrium. The density in the tidal stream, and hence the mass transfer rate, is determined by the placement of the stellar surface relative to the L1 point (an arbitrary boundary condition in our model). Both the width of, and the density in, the tidal stream decrease as the stream accelerates toward the compact object.

By the end of the simulation the accretion disk has relaxed into a roughly steady-state configuration. The accretion flow has fully circularized and is nearly Keplerian, the vertical density profile matches that of an isothermal steady-state disk, and the outer radius is truncated at $\sim 8 \times 10^{10}$ cm, corresponding to $\sim 70\%$ of the Roche lobe of the compact object. Note, however, that the mass flux through the disk is not in equilibrium - even if such an equilibrium were possible in this numerical model, it would take far too long to reach.

The outer edge of the disk has a scale height of $\sim 2 \times 10^9$ cm, although the disk is somewhat thinner on the side nearest the primary star and fatter on the far side. This scale height is consistent with that of an isothermal accretion disk in steady state (the sound speed of the cold disk gas in our model is $c_s = 2.136 \times 10^6$ cm s^{-1}). The width of the tidal stream in the vicinity of the disk edge is noticeably wider, with a scale height of order $\sim 3 \times 10^9$ cm. As a result, a significant fraction of the tidal stream gas is not stopped at the disk edge, but rather flows over and under the disk along its surface. This stream overflow ultimately merges with the accretion disk in the vicinity of the point of closest approach: the location at which a ballistic trajectory from the L1 point would reach the closest to the compact companion.

In addition to the impact by the tidal stream, the outer edge of the disk is continually ablated by the strong stellar wind from the primary star. Note that this equatorial wind is enhanced by the wind compressed disk effect, and it is not directly affected by the X-ray source since it is shadowed by the accretion disk. As a result, the equatorial wind is strong enough to ablate a significant mass flux off the edge of the disk, particularly on the back side as seen in Figure 3. Furthermore, the ram pressure of this equatorial wind inflates the outer edge of the disk, creating a small outer rim that extends higher than the rest of the disk.

Although the outer regions of the disk are sufficiently resolved by our numerical grid, the inner regions of the disk are not. The scale height of a steady isothermal disk at a disk radius of 1.5×10^{10} cm should be $\sim 2.6 \times 10^8$ cm, but the limited resolution of our numerical model limits the disk thickness to values approximately three times larger. This limitation has direct bearing on the results of this paper in that this poor numerical resolution effectively limits (through the high opacity of the disk material) the cone of X-rays to a smaller opening angle than if the disk was adequately resolved at small disk radii.

The intense X-ray luminosity of the accreting compact companion can influence the circumstellar gas in many ways, but in this numerical model the dominant effect is a strong bipolar wind driven off the inner region of the accretion disk via X-ray irradiation. The dense, cool gas on the surface of the accretion disk is heated by the incident X-ray flux to several million Kelvins. The ensuing high thermal pressure drives a strong wind with velocities reaching 2000 km s^{-1}. This irradiation is so intense in this numerical model that the X-ray flux striking the inner disk edge completely ablates the inner disk, leav-

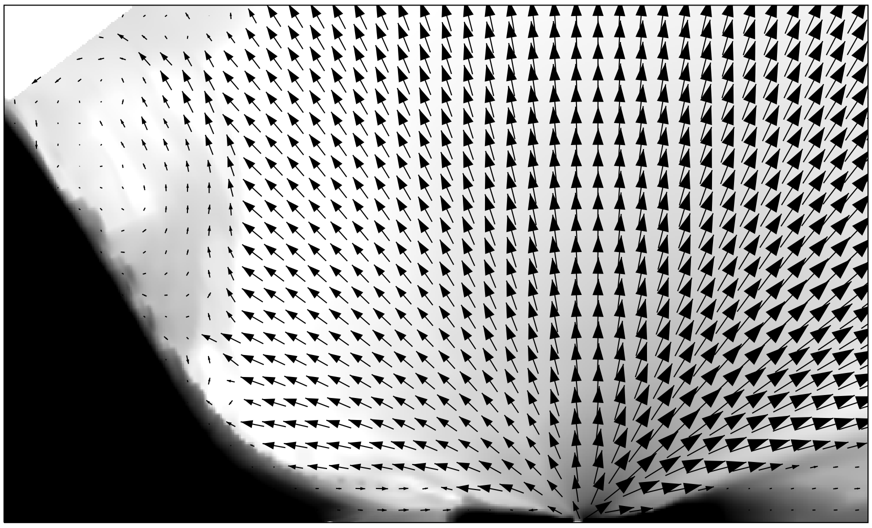

Figure 4: The bipolar disk wind emanating from the inner region of the accretion disk is evident in this two-dimensional slice along the line of centers of the binary system. Note that the disk wind crashes into an irradiation-driven wind off the surface of the primary star.

ing a substantial hole. As seen in Figure 4, this disk wind is roughly spherical. This has the interesting effect of producing a large volume of X-ray heated gas with a roughly constant ionization parameter. Since both the gas density and X-ray flux are decreasing as the square of the distance from the X-ray source, the ionization parameter in this gas remains at a constant value.

Because the poor numerical resolution in the inner accretion disk affects the vertical structure of the disk, the conservation of angular momentum in the disk gas, and the thermal transition of the X-ray heated gas, the geometry and mass flux in this bipolar wind is very uncertain. Nonetheless, it is clear from both simple order of magnitude estimates and from detailed calculations (de Kool & Wickramasinghe 1999) that the intense X-ray flux present in X-ray binaries will drive a substantial mass loss from the accretion disk.

Due to the shadowing effects of the accretion disk, the effects of X-ray photoionization are restricted to the bipolar disk wind in this model. Gas outside of the disk wind is shielded from the X-ray source, and as a result, there is no independent photoionization wake visible in this model. Instead, there is a relatively dense wake of circumstellar gas piled up along the leading surface separating the disk wind and the stellar wind. This modest wake, with a density contrast of ~ 4, can be seen in the horizontal slices shown in Figure 5.

As seen in Blondin & Woo (1995), the radiatively-driven wind of the primary star is replaced by a thermally driven wind on the X-ray irradiated face of the primary. The high X-ray flux on the irradiated surface is strong enough to supress the radiative driving force and quench the normal radiatively driven stellar wind. Instead, the X-ray flux heats the outer atmosphere of the star up to X-ray temperatures, and the ensuing high thermal pressure drives an outflow off the stellar surface. In this particular model, however, the thermally-driven stellar wind is effectively snuffed by the disk wind. The momentum in the disk wind is sufficiently high that it stops the stellar wind before it can reach a sonic point. This subsonic outflow is then redirected up over the top of the star along with the supersonic disk wind. This dynamical interaction between star and disk winds can be seen in Figure 4.

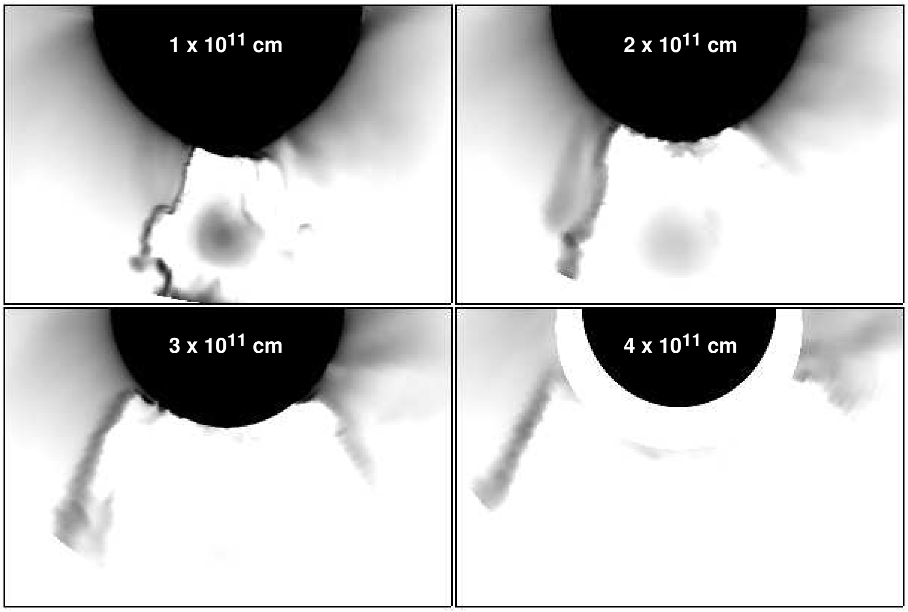

Figure 5: The influence of the disk wind on the circumstellar structure is seen in these two-dimensional slices parallel to the equatorial plane. The density in the leading wake (left of the disk wind) is 4 times higher than the normal stellar wind at that radius. Note that in the top slice the inner edge of the grid is beyond the surface of the primary star.